SUPPLEMENTARY INFORMATION

NOTE: In the supplement, like in the main manuscript, we refer to COUP-TFII as 'NR2F2'.

A. SUPPLEMENTAL DATA

Figure S1. *Nr2f2* is expressed in vECs and LECs in zebrafish and *Xenopus*

A-C. Whole-mount in situ hybridization (WISH) on 48 hpf (A,B) or 6 dpf (C) zebrafish (z) showing *znr2f2* expression in the posterior cardinal vein (PCV: arrowheads in B and lower luminal structure in inset ('i')1), the parachordal lymphangioblast (PL) string (a bilateral structure at notochord (NC) level; arrowheads in i2) and the thoracic duct (TD; arrowhead in i3) in addition to its expression in the neural tube (NT). Note lack of expression in the dorsal aorta (DA). ***D.*** WISH on stage (ST)40 *Xenopus* tadpoles revealing *xnr2f2* expression in the PCV and the ventral caudal lymphatic vessel (VCLV), but not in the DA. ***E.*** After specifically labeling LECs with red fluorescent TRITC-dextran (shown in the inset where VCLV ECs appear yellow) in ST45 *Tg(Flk1:eGFP)* tadpoles, $TRITC^{+}GFP^{+}$ LECs (enriched for LEC markers *prox1* and *flt4*; yellow bars) and $TRITC^{-}GFP^{+}$ blood vascular ECs (BECs; green bars) were sorted and assayed by qRT-PCR. Data expressed as % relative to the expression in the GFP^{-} non-EC fraction (simultaneously sorted with the other fractions) represent the mean ± SEM of 7-10 independent sorting experiments (**P*<0.05; ***P*<0.01 vs. BECs). Scale bars: 25 μm in A,C,D; 100 μm in B and 200 μm in E (inset).

Figure S2. zNR2F2 knockdown causes cardiovascular defects

A. Schematic representation of the vasculature in a 48 hpf zebrafish (*Danio rerio*) embryo. ***B.*** Detail of the heart region, showing in the right panel pericardial edema (indicated by arrowhead) in a 48 hpf embryo treated with zebrafish (z)$NR2F2^{ATG}$ morpholino (Mo). ***C.*** Detail of the major trunk vessels (dorsal aorta or DA in red and posterior cardinal vein or PCV in blue). The lower-left cross-section of a 48 hpf *Tg(Fli1:eGFP)*^{y1} embryo treated with non-silencing ('ns') Mo reveals normal segregation of DA and PCV, while the lower-right image of a 48 hpf *Tg(Fli1:eGFP)*^{y1} embryo treated with zNR2F2 Mo shows fusion of both major trunk vessels. DAPI (blue) is used as nuclear counterstain. ***D.*** Detail of the intersomitic vessels (ISV). The lower-left confocal image of a 48 hpf *Tg(Fli1:eGFP)*^{y1} embryo treated with ns Mo reveals normal anatomy of the ISV, while the lower-right confocal image of a 48 hpf *Tg(Fli1:eGFP)*^{y1} embryo treated with zNR2F2 Mo shows abnormal branching of the ISV. ***E.*** Detail of the vascular labyrinth in the tail region. The lower-left confocal image of a 48 hpf *Tg(Fli1:eGFP)*^{y1} embryo treated with ns Mo reveals normal anatomy of the vascular

labyrinth, while the lower-right confocal image of a 48 hpf *Tg(Fli1:eGFP)*^{y1} embryo treated with zNR2F2 Mo shows abnormal vessel composition in the vascular labyrinth. ***F.*** Quantification of the cardiovascular defects as a function of zNR2F2 Mo dose. Data represent % incidence of defects (**P*<0.0001, ***P*=0.0011 vs. ns). The number of embryos analyzed is mentioned in the bottom row. Scale bars: 10 μm in C; 200 μm in D and 400 μm in B,E.

Figure S3. Scoring of lymphatic phenotype upon xNR2F2 knockdown

A. The top panel represents a schematic of the main vascular structures in stage (ST)45 *Xenopus* tadpoles (blood vessels are in blue, dorsal aorta or DA is highlighted in red). For evaluation of the lymphatic vessels in *Xenopus Tg(Flk1:eGFP)* tadpoles, the eGFP^{+} main lymphatic vessels in the trunk region (the dorsal and ventral caudal lymphatic vessel or DCLV and VCLV, respectively, shown in green) were evaluated. Since the severity of the phenotype was different along the anterior-posterior axis, anterior and posterior trunk regions were scored separately for the (partial) absence or abnormalities of DCLV or VCLV. The lower insets show the quantitative analysis of the phenotype in the anterior region (left) or posterior region (right) revealing a dose-dependent effect of *Xenopus* (x)NR2F2 morpholino (Mo) as compared to the non-silencing ('ns') Mo- treated tadpoles on the presence/disorganized structure of the DCLV (left diagram) and the VCLV (right diagram). Numbers on top of the bars indicate the numbers of tadpoles analyzed (**P*<0.0001 vs. ns Mo for each of the xNR2F2 Mo doses). ***B-E.*** Representative confocal images of the anterior portion of the trunk of ST45 *Tg(Flk1:eGFP)* tadpoles injected with ns (B,C = inset*)* or xNR2F2 Mo (D,E = inset) showing absence (asterisks in D) of large parts of the dorsal caudal lymphatic vessel (DCLV) or disorganized structure (E) of the ventral caudal lymphatic vessel (VCLV). Tadpole head facing left and dorsal side facing up in B-E. Scale bars: 200 μm in C,E; 250 μm in B,D.

Figure S4. Endothelial cell sorting from zebrafish embryos

A. <u>*Pre-sort diagrams.*</u> Forward scatter (FSC)/side scatter (SSC) diagrams of monocellular suspensions of AB (*i*) or *Tg(Fli:eGFP)*^{y1} (*iii*) 48 hpf zebrafish embryos gated ('G1') for live singlets and the corresponding histograms for eGFP signal, revealing absence of the signal in AB embryos (*ii*) and 5.2 % eGFP^{+} (Fli^{+}) endothelial cells in *Tg(Fli:eGFP)*^{y1} embryos (*iv*). ***B.*** <u>*Post-sort analysis.*</u> Histograms of the sorted non-endothelial (Fli^{-}; *i*) and endothelial (Fli^{+}; *ii*) fractions of *Tg(Fli:eGFP)*^{y1} 48 hpf embryos revealing the high purity of the sorted populations. Diagram (*iii*) represents qRT-PCR analysis on the sorted fractions showing

significant enrichment of endothelial genes (*fli*, *cdh5* and *kdra*) in the endothelial (Fli^+; red bars) fraction and significant enrichment for *dlb*, a non-endothelial marker in the non-endothelial (Fli^-; blue bars) fraction. Data expressed as % expression versus total zebrafish RNA, represent the mean ± SEM of three independent sorts (**P*<0.05 vs. the other fraction).

Figure S5. Endothelial cell sorting from *Xenopus* tadpoles

A. Fluorescent image of the trunk region of a stage (ST)45 *Tg(Flk1:eGFP) Xenopus* embryo (both lymphatic and blood vessels are GFP+) injected 1 day earlier with red TRITC-dextran. The bottom picture zooms in on the posterior cardinal vein (PCV) and the ventral caudal lymphatic vessel (VCLV) revealing specific TRITC labeling of the lymphatic endothelial cells (LECs) of the VCLV (in yellow). ***B.*** The FACS dot plot shows the sorting set-up for isolating $TRITC^+eGFP^+$ LECs and $TRITC^-eGFP^+$ blood vascular endothelial cells (BECs). ***C.*** Diagram represents qRT-PCR analysis on sorted BECs, LECs and non-ECs ($eGFP^-$) fractions revealing significant enrichment for EC marker *flk1* in both BEC (green bars) and LEC (yellow bars) fractions compared to the non-EC fraction (red bars) and enrichment for LEC markers (*prox1* and *flt4*) in the LEC fraction vs. the BEC and non-EC fractions. Data expressed as % vs. non-ECs represent the mean ± SEM of 7-10 independent sort experiments. (**P*<0.05, ***P*<0.01 vs. non-ECs or BECs). Scale bars: 200 μm in A.

B. SUPPLEMENTAL EXPERIMENTAL PROCEDURES

Morpholino knockdown in zebrafish and *Xenopus* embryos

Antisense morpholino oligonucleotides (morpholinos) targeting either the translational initiation site (X^{ATG}) or the first exon-intron boundary (X^{Spl}) of *nr2f2* (GenBank ID: NM_131183.1 for zebrafish and NM_001087019.1 for *Xenopus laevis*) and standard control morpholinos were purchased from Gene Tools (LLC, Corvallis). Sequences are listed in the table below. Various doses (as indicated) of morpholinos were injected into single- to two-cell stage zebrafish embryos or in two-cell stage frog embryos, using procedures as previously described [1,2].

List of morpholinos

Gene name	Morpholino sequence	Reference
NR2F2^{ATG}*	ATG morpholino, zebrafish; 5' AGCCTCTCCACACTACCATTGCCAT 3'	Gene Tools, LLC
NR2F2^{Spl}*	splice site morpholino, zebrafish; 5' ACAAAAATCCGAATACCTTCCCGTC 3'	Gene Tools, LLC
Non-silencing	zebrafish and *Xenopus* 5' CCTCTTACCTCAGTTACAATTTATA 3'	Gene Tools, LLC
NR2F2^{ATG}**	ATG morpholino, *Xenopus*; 5' ACGCACCCACTACCATTGCCATATC 3'	Gene Tools, LLC

*also known as seven-up(40) [3]; **also known as xCOUP-TFB [4].

Scoring of prox1 WISH in morpholino-injected *Xenopus* embryos

Analysis of LEC commitment and migration on tadpoles processed for *prox1* whole-mount in situ hybridization was performed as previously described [2]. Briefly, maximal migration distance (MMD) from the posterior cardinal vein in dorsal direction was measured, in addition to the area occupied by *prox1*$^+$ cells in three defined regions: area 1 (an estimate for commitment and corresponding to the region between the ventral border of the trunk and the dorsal margin of the endoderm) and area 2 and 3 (estimates for migration, corresponding to the area between the dorsal margin of the endoderm and the floor plate of the neural tube and the area between the floor plate and the dorsal roof, respectively). All phenotyping data are pooled data from at least 3 independent experiments, with analysis of between 7 and 40 injected embryos per condition.

List of probes for whole-mount in situ hybridization

Gene name	Species	GenBank ID [Reference]
nr2f2	zebrafish and *Xenopus*	NM_131183
ephb4a	zebrafish	NM_131414
flt4	zebrafish	NM_130945 [5]
ephrinb2a	zebrafish	NM_131023 [6]
gridlock	zebrafish	NM_131622.2
prox1	*Xenopus*	NM_001090703.1 [2]

List of primers for qRT-PCR

Gene name	Species	Fwd primer sequence (5'-3')	Rev primer sequence (5'-3')
ephrinb2a	Z	GTGAAAACCAAGTCGATGAAAATCA	GAGGGTAACTGGTAGGGTAGTCTTTG
ephb4a	Z	TCGCTCTAAACCTGAGTGGGA	CACGTACACCTGTGATGCCC
gridlock	Z	GGCTCACCTACAACGACATCC	CCAACTTGGCAGATCCCTGT
prox1a	Z	GCGCAAAAGCAACCTTTCTT	CTGCACCACTGAACACTCAACA
prox1b	Z	CGACCCCTCTCCATCAGATA	GCGCGTGTAGAAGAACATGA
ef1α	Z	TCACTGGTACTTCTAGGCTGACT	TTCTTGGAGATACCAGCCTCAAA
flt4	Z	CTGTCGGATTTGGATTGGGA	GGTGGACTCATAGAAAACCCATTC
fli1	Z	CCGAGGTCCTGCTCTCACAT	GGGACTGGTCAGCGTGAGAT
cdh5	Z	TGTTCAAGCCAAAGACATGC	TTTCACTTCCGGGTTTCAAG
kdra	Z	ACTTTGAGTGGGAGTTTCATAAGGA	TTGGACCGGTGTGGTGCTA
dlb	Z	CGCTGTAGCCACAAACCATGT	CGAGAGCCGCTGAAACCA
nr2f2	X	AAGCGAAGTGTAAGGCGAAA	CTGGCTGCCAAATCTAGAGG
flk1	X	TGAATTTGTGTTATACAAGCCGAA	AGCGCCTCTTAAGGTCTCCTTGA
prox1	X	GTCGGAGTGCGGAGACATG	GGCCTTTTTCAAGTGATTTGGA
flt4	X	CCCCAGCCCTCATTCCA	GCTGGGACTGACGATATTTGC
ef1α	X	GAACCATCGAAAAGTTCGAGAAG	TCCAAGACCCAGGCATACTTG

Abbreviations: Fwd: forward; Rev: reverse; Z: zebrafish; X: *Xenopus*

C. REFERENCES IN SUPPLEMENT

[1] I. Geudens, R. Herpers, K. Hermans, I. Segura, C. Ruiz de Almodovar, J. Bussmann, F. De Smet, W. Vandevelde, B.M. Hogan, A. Siekmann, F. Claes, J.C. Moore, A.S. Pistocchi, S. Loges, M. Mazzone, G. Mariggi, F. Bruyere, F. Cotelli, D. Kerjaschki, A. Noel, J.M. Foidart, H. Gerhardt, A. Ny, T. Langenberg, N.D. Lawson, H.J. Duckers, S. Schulte-Merker, P. Carmeliet, and M. Dewerchin, Role of delta-like-4/Notch in the formation and wiring of the lymphatic network in zebrafish, Arterioscler. Thromb. Vasc. Biol. 30 (2010) 1695-702.

[2] A. Ny, M. Koch, M. Schneider, E. Neven, R.T. Tong, S. Maity, C. Fischer, S. Plaisance, D. Lambrechts, C. Heligon, S. Terclavers, M. Ciesiolka, R. Kalin, W.Y. Man, I. Senn, S. Wyns, F. Lupu, A. Brandli, K. Vleminckx, D. Collen, M. Dewerchin, E.M. Conway, L. Moons, R.K. Jain, and P. Carmeliet, A genetic Xenopus laevis tadpole model to study lymphangiogenesis, Nat. Med. 11 (2005) 998-1004.

[3] S.Y. Tsai, and M.J. Tsai, Chick ovalbumin upstream promoter-transcription factors (COUP-TFs): coming of age, Endocr. Rev. 18 (1997) 229-40.

[4] J. van der Wees, P.J. Matharu, K. de Roos, O.H. Destree, S.F. Godsave, A.J. Durston, and G.E. Sweeney, Developmental expression and differential regulation by retinoic acid of Xenopus COUP-TF-A and COUP-TF-B, Mech. Dev. 54 (1996) 173-84.

[5] M.A. Thompson, D.G. Ransom, S.J. Pratt, H. MacLennan, M.W. Kieran, H.W. Detrich, 3rd, B. Vail, T.L. Huber, B. Paw, A.J. Brownlie, A.C. Oates, A. Fritz, M.A. Gates, A. Amores, N. Bahary, W.S. Talbot, H. Her, D.R. Beier, J.H. Postlethwait, and L.I. Zon, The cloche and spadetail genes differentially affect hematopoiesis and vasculogenesis, Dev. Biol. 197 (1998) 248-69.

[6] J. Chan, J.D. Mably, F.C. Serluca, J.N. Chen, N.B. Goldstein, M.C. Thomas, J.A. Cleary, C. Brennan, M.C. Fishman, and T.M. Roberts, Morphogenesis of prechordal plate and notochord requires intact Eph/ephrin B signaling, Dev. Biol. 234 (2001) 470-82.

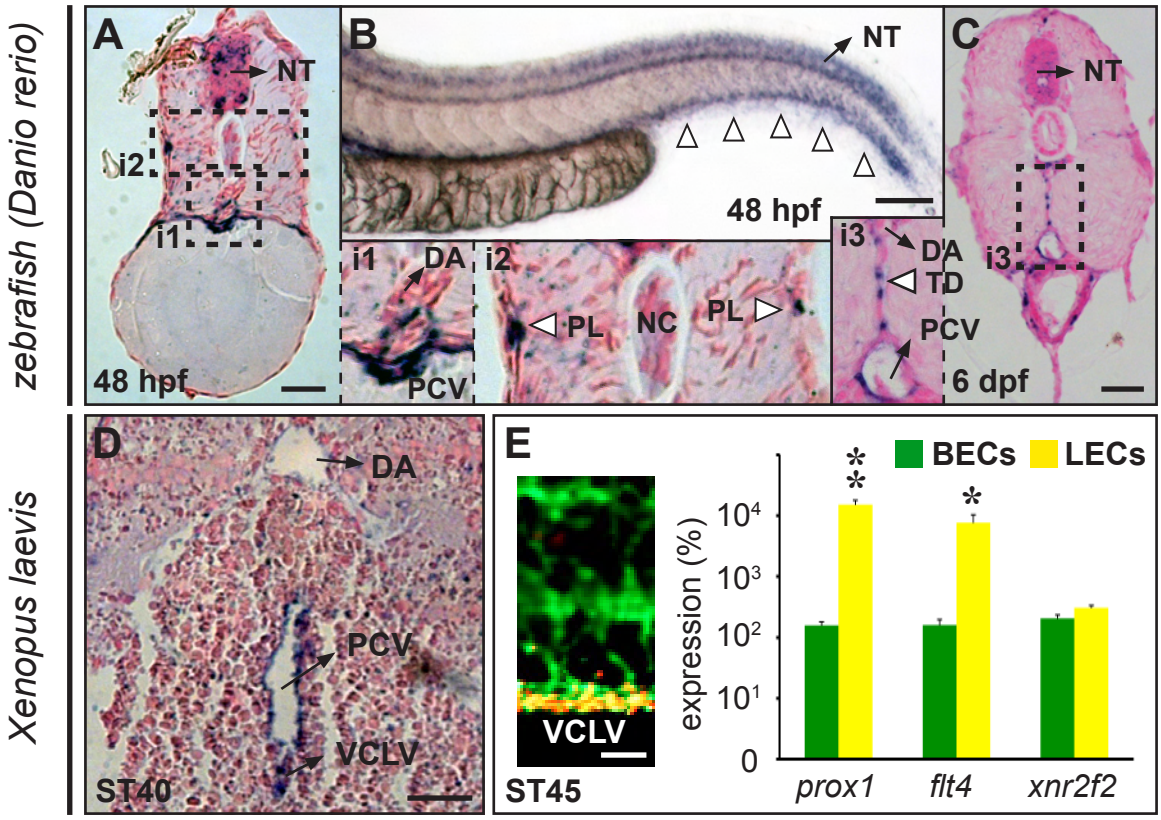

Aranguren *et al.* Figure S1

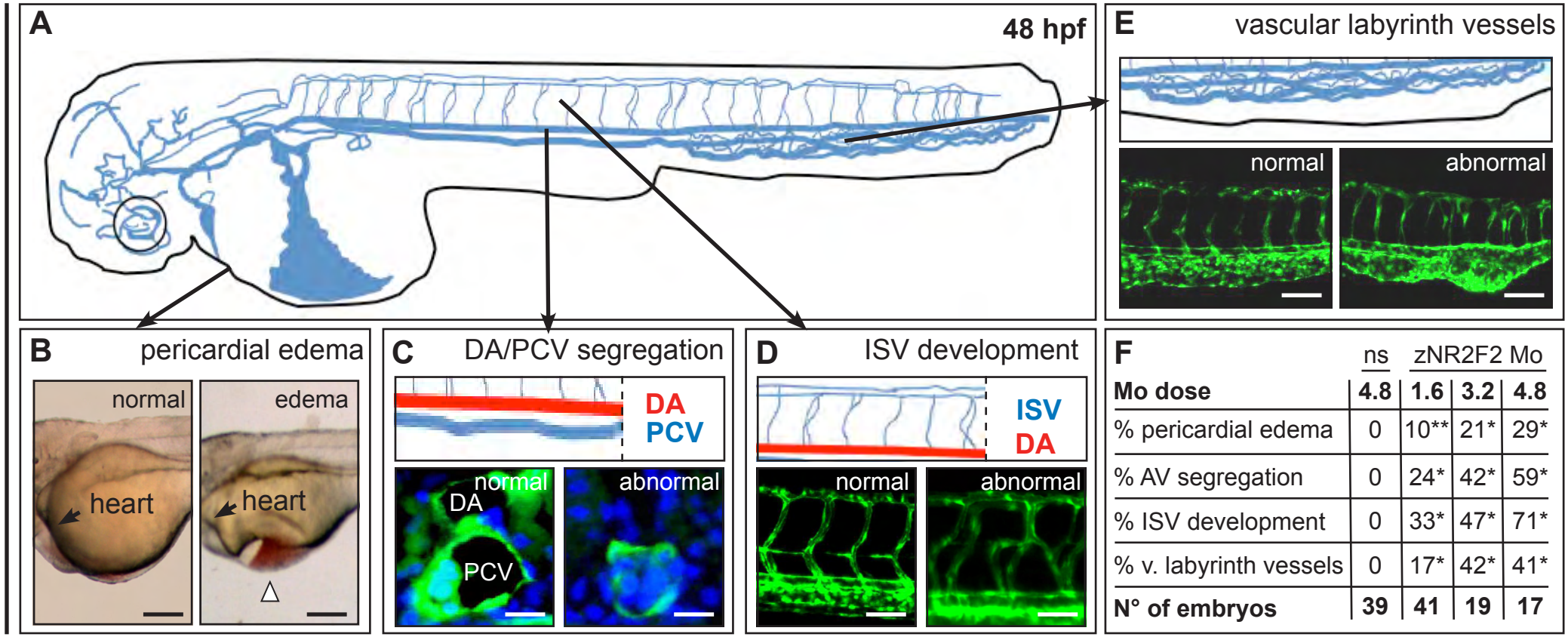

F

	ns	zNR2F2 Mo		
Mo dose	**4.8**	**1.6**	**3.2**	**4.8**
% pericardial edema	0	10**	21*	29*
% AV segregation	0	24*	42*	59*
% ISV development	0	33*	47*	71*
% v. labyrinth vessels	0	17*	42*	41*
N° of embryos	**39**	**41**	**19**	**17**

Aranguren *et al.* Figure S2

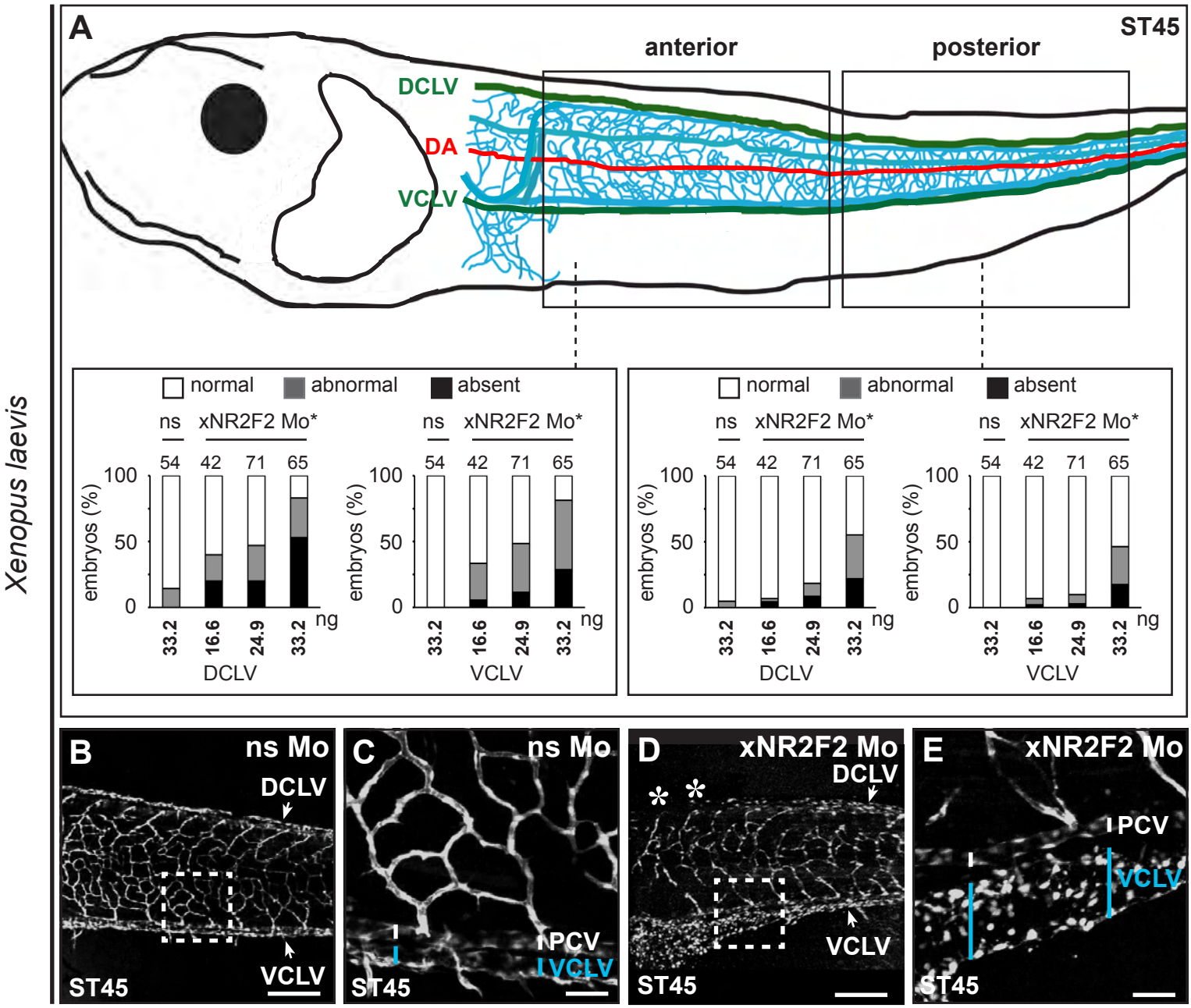

Aranguren *et al.* Figure S3

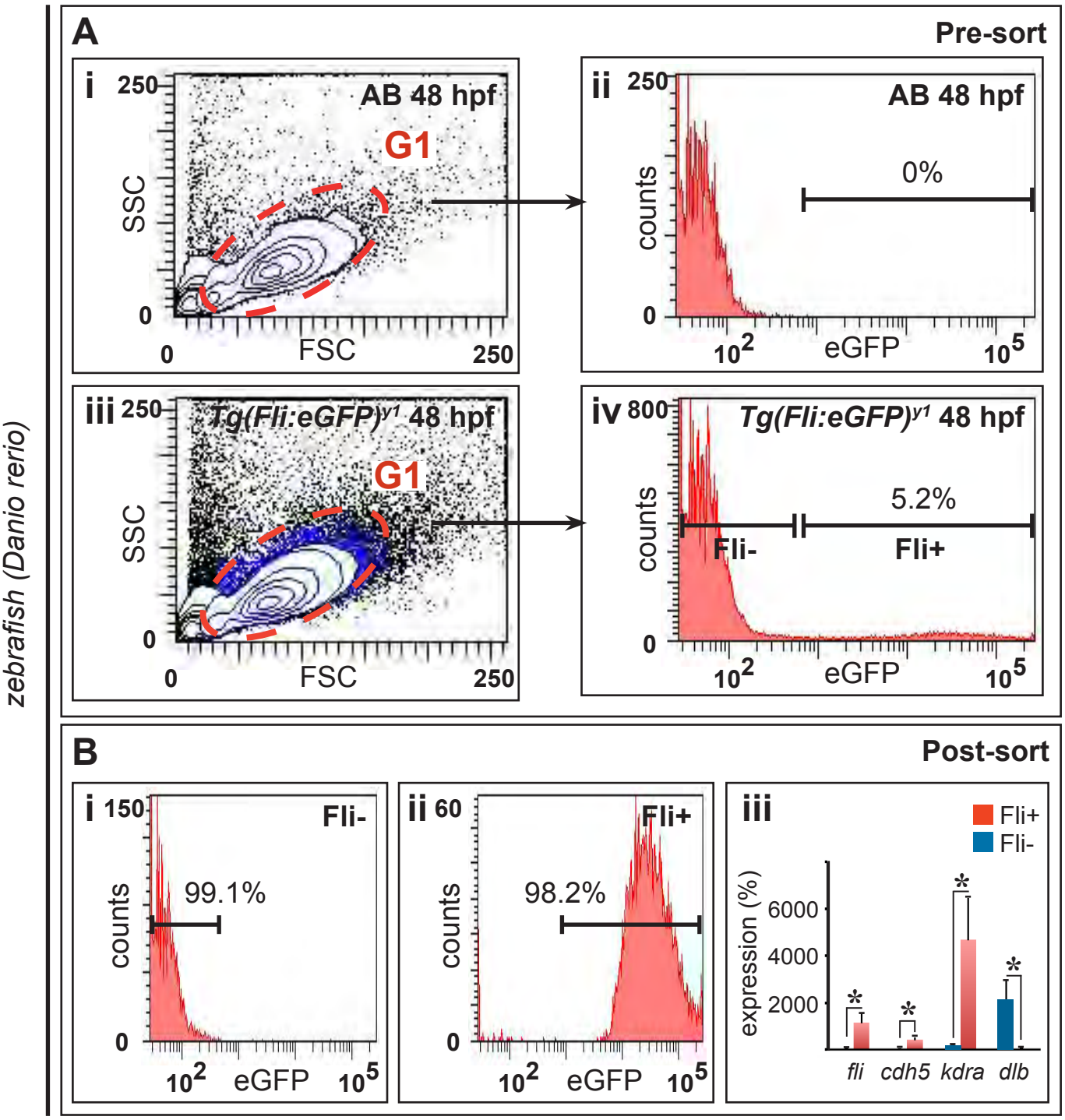

Aranguren *et al.* Figure S4

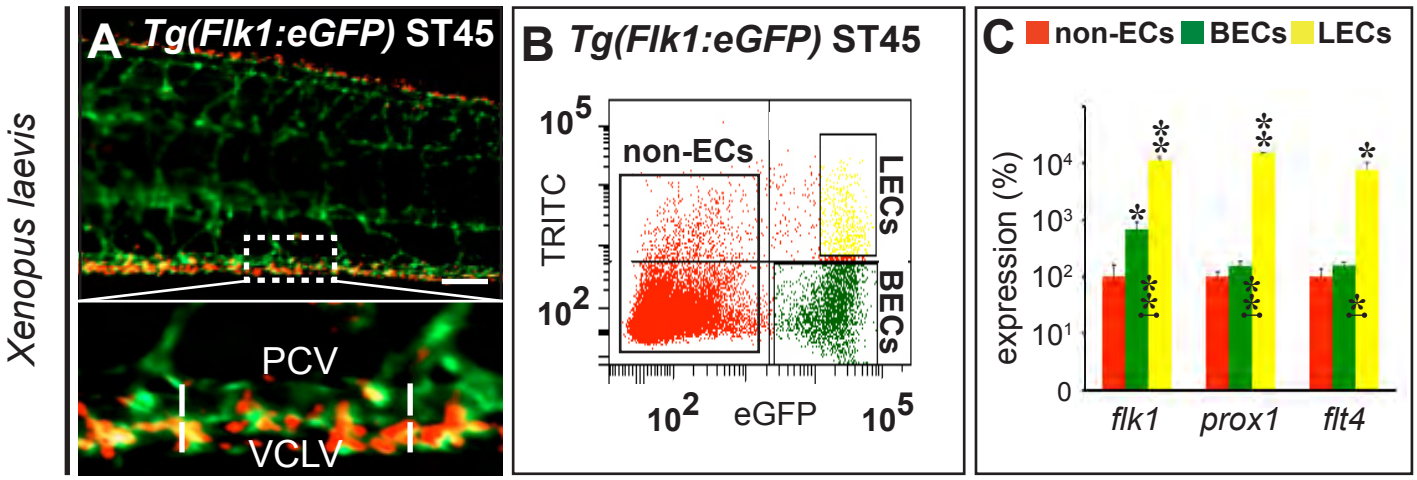

Aranguren *et al.* Figure S5